hydrocarbon side chains are not perpendicular to the monolayer plane. This is known from 62-Å $d$ spacing obtained from X-ray diffraction of built-up monomeric Li salt bilayers (multilayers). From the theoretical monomer bilayer thickness of 74 Å, a tilt angle of 57° is obtained (57° between the monolayer plane and the hydrocarbon axis). In considering a reasonable structure for the monomer, it can be assumed that the axes of the hydrocarbon side chains are parallel to one another (as in all forms of polyethylene[8] and low molecular weight paraffins[9]) for energetic reasons. To have all the hydrocarbon axes parallel and preserve the glide-plane symmetry along $b$, the tilt of the chains (with respect to the monolayer plane) must be toward the $b$ axis (making $c$ a unique axis).

As indicated by optical microscopy, the $\theta$ value (the angle between the planar zigzag and the $b$ axis) is probably on the order of 50°.[3]

A monomeric structure with a tilt angle of 57° toward $b$ and a 50° value of $\theta$ could only polymerize to the polymer structure as indicated below, where only the diacetylene rods and planar zigzags are represented.

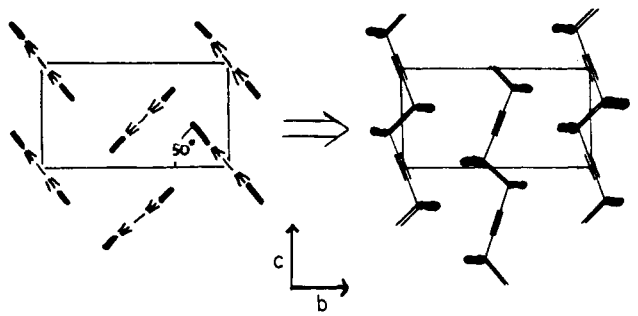


The resulting polymer has a glide-plane symmetry along $b$ which is identical with that in Figure 7, right, and is a good indication that this is the actual polymer structure.

## Conclusions

The results presented in this paper, when taken together with those previously reported,[1-3] clearly indicate that the polymerization reaction proceeds in the monomer phase indicated above. A phase change from the monomer structure to the glide-related polymer structure occurs after appreciable conversion.

**Acknowledgment.** Support of this work under National Science Foundation Grant DMR-77-13001-A01 is gratefully acknowledged.

## References and Notes

(1) Day, D. R.; Ringsdorf, H. *J. Polym. Sci., Polym. Lett. Ed.* **1978**, *16*, 205.
(2) Day, D. R.; Ringsdorf, H. *Makromol. Chem.* **1979**, *180*, 1059.
(3) Day, D. R.; Lando, J. B. *Macromolecules*, preceding paper in this issue.
(4) Day, D. R.; Lando, J. B., submitted to *J. Polym. Sci., Polym. Phys. Ed.*
(5) Doyle, P. A.; Turner, P. S. *Acta Crystallogr., Sect. A* **1968**, *24*, 390.
(6) Stout, G.; Jenson, L. "X-Ray Structure Determination"; Macmillian: New York, 1968.
(7) Woolfson, M. N. "X-Ray Crystallography"; Cambridge University Press: New York, 1970.
(8) Yemni, T.; McCullough, R. L. *J. Polym. Sci., Polym. Phys. Ed.* **1973**, *11*, 1385.
(9) Kitaigordoskii, A. I. *Sov. Phys.—Crystallogr.* **1957**, *2*, 454.

# Copolymer Structure through Charge Injection and X-ray Photoemission

**T. J. Fabish* and H. R. Thomas**

*Xerox Corporation, Rochester, New York 14644.* *Received January 21, 1980*

ABSTRACT: X-ray photoemission and contact-charge injection experiments are applied to random styrene/methyl methacrylate and random and block styrene/2-vinylpyridine copolymer systems as well as to the homopolymers to investigate the electronic structures of the copolymers. The lowest energy electronic excitations and the observable polymer charge state distributions are governed by the electronic structures of the phenyl, ester, and pyridine pendent groups in these polymers, and their individual responses are easily discernible experimentally. Hence, preservation of the characteristic pendent-group responses in the random Sty/MM copolymer indicates that an insignificant perturbation occurs in the constituent moieties at a molecular level and for all copolymer molar ratios. This is not the case for random Sty/2VP wherein a strong pendent-group interaction takes place which significantly alters features of the XPS spectrum and the copolymer charge-state distribution. The thermodynamic drive for the interaction is discussed in terms of chemical potential values deduced from the homopolymer charge-state distributions. In contrast, the block Sty/2VP copolymer exhibits superposition of the characteristic constituent responses similarly to random Sty/MM. However, superposition occurs in this case because the thermodynamically favored pendent-group interaction is limited in extent by the formation of essentially homopolymer domains in this incompatible block system. The electronic response of the block Sty/2VP copolymer is observed to exhibit a pronounced dependence on the thermal history of the film, and rather persistent solvent effects may be present. These results emphasize the importance of electronic interactions, geometrical constraints, and film-forming technique in determining the electronic properties (and surface composition) of copolymers.

## Introduction

Recent experimental[1,2] and theoretical[3-7] investigations of saturated carbon chain polymers have shown how large pendent groups can provide localization sites (charge states) for excess charge carriers in the solid created, say, upon carrier injection during contact with another material or by ejection of an electron in a photon-assisted emission event. Moreover, large pendent groups tend to dominate the lowest energy neutral (excitonic) electronic excitations[5-7] as well as those associated with charge states. The prominence of the pendent groups in neutral and charged excitation processes occurs because the molecular orbitals

* Present address: Ashland Chemical Company, Columbus, Ohio 43216.

0024-9297/80/2213-1487$01.00/0 

of the pendent group often provide the frontier eigenstates of the charge–neutral polymer solid that form the parentage of the final, relaxed molecular ion states.

The understanding of the origin of molecular ion states in polymers provided by recent theory and the clear visibility of the pendent groups in contact-charge injection[1,2,8] and photoemission[7,9] experiments offer sensitive means for studying homopolymer and copolymer surface and bulk electronic structures. These techniques are applied herein to two copolymer systems, styrene/methyl methacrylate (Sty/MM) and styrene/2-vinylpyridine (Sty/2VP), to obtain information about surface composition and pendent-group interactions. It will be shown that, in the Sty/MM system, the distinguishing phenyl and ester groups behave sufficiently independently in the random copolymer configuration to allow a description of the lowest energy responses of the copolymer at all Sty/MM ratios in terms of a molar-weighted superposition of the homopolymer responses. This is found not to be the case for the random (46/54) Sty/2VP copolymer, whose response is found to be closely similar to one of the homopolymers, P2VP. For the block 53/47 Sty/2VP copolymer, however, superposition is again observed. The differences are discussed in terms of pendent-group interactions and configuration-imposed geometric constraints on the interaction. Finally, comparisons of surface-sensitive and bulk-sensitive experimental results give indications of pendent-group orientations at the polymer/vacuum interface in two of the three homopolymers considered. The preferential surface alignments persist in the copolymer systems where superposition occurs.

## X-ray Photoemission Spectroscopy

**A. Experimental Procedure.** Angular-dependent X-ray photoelectron spectroscopy, XPS($\theta$), was used to determine the surface composition and topography of a series of polystyrene–poly(methyl methacrylate) (Sty/MM) random copolymers and polystyrene–poly(2-vinylpyridine) (Sty/2VP) random and block copolymers.

In the XPS experiment, one measures the binding energies of electrons ejected by the interaction of a molecule with a monoenergetic beam of soft X-rays.[10] Information about the surfaces of solids is derived from measurements of the absolute binding energies, relative kinetic energies, and peak intensities corresponding to the direct photoionization of the core levels. XPS is inherently sensitive to the surfaces (top few monolayers)[10] of solids because of the very short (<100 Å) mean free paths for electrons and their strong dependence on kinetic energy.[11-14] By coupling our knowledge of electron mean free paths in polymers with measurements of the angular dependence of the photoelectron spectra, XPS($\theta$), it is possible to depth profile surface compositional variations and to model the morphology of polymer surfaces.[9] Experimentally, the XPS($\theta$) measurements are made by rotating the sample relative to the fixed-position electron analyzer and this, in effect, varies the sampling depth. The sampling depth is maximized when the electrons are collected normal ($\theta$ = 0) to the sample surface, and minimized as $\theta \rightarrow 90°$. For $C_{1s}$ electrons excited by $Mg_{K\alpha_{1,2}}$ radiation, the inelastic mean free path is ~15 Å[14] and, therefore, about 95% of the signal arises from the top 50 Å at $\theta$ = 0° and from the top 10 Å at $\theta$ = 80°. Thus, by taking spectra at angles ranging from 0 to 80°, one can determine the average composition at each effective sampling depth and establish a composition depth profile in the outermost 50 Å of the sample. (Although the value of 15 Å for the inelastic mean free path used here was originally determined on poly(*p*-xylylene),[14] it is assumed this value will differ little for the systems of present interest.)

XPS sample preparation consisted of dip-coating thin films (~5 $\mu$m) of the copolymers onto flat aluminum substrates from dilute, spectroscopic grade chloroform and tetrahydrofuran solutions. The films were dried in an argon atmosphere at ambient temperature to discourage surface oxidation of the copolymers and heated above the polymer $T_g$, in the spectrometer for 1 h prior to measurement. The $Cl_{2p}$ or $O_{1s}$ core levels were monitored to ensure all residual solvent was removed from the film before the XPS study was begun.

Spectra were recorded on an AEI ES200B spectrometer by using $Mg_{K\alpha_{1,2}}$ exciting radiation. Typical operating conditions were as follows: X-ray gun, 12 kV, 15 mA; pressure in the source chamber ca. $10^{-8}$ torr. Under the experimental conditions employed, the gold $4f_{7/2}$ level at 84-eV binding energy (BE) used for calibration had a full width half-maximum (fwhm) of 1.2 ± 0.1 eV. No evidence was obtained for radiation damage to the sample from long-term exposure to the X-ray beam. Due to the rather long analysis times required for the angular-dependent studies, a liquid nitrogen cooled X-ray cap was used throughout the study to eliminate hydrocarbon contamination of the sample surface.[15]

Calibration of the absolute energy scale was achieved by disconnecting the liquid nitrogen cooling cap on the X-ray anode and allowing hydrocarbon contamination to collect on the sample surface. The value of 285.0 eV was used for the $C_{1s}$ core level of the hydrocarbon contaminant. The details of this method of calibration have been discussed elsewhere.[13]

Overlapping peaks were resolved into their individual components by use of a Du Pont 310 curve resolver. The detailed deconvolutions were based on a knowledge of line widths determined from studies of homopolymers and model compounds.[16] These studies have shown Gaussian line shapes for individual components of the core-level spectra for $C_{1s}$ and $N_{1s}$ levels.

**B. Results.** The XPS spectra of the PS, PMMA, and P2VP homopolymers for normal exit ($\theta$ = 0) are given in Figures 1 and 2. These spectra provide the basis for interpretation of the copolymer spectra included in Figures 1 and 2.

Consider first the PS and P2VP homopolymer spectra of Figures 1 and 2. Although the $C_{1s}$ core level responses are quite similar for the two homopolymers, major differences appear in the $N_{1s}$ core level peak associated with P2VP, and in the intensities and line shapes of the $\pi^* \leftarrow \pi$ shake-up peaks of the two polymers.

Details of the PMMA spectrum (Figure 1) clearly distinguish this polymer from PS and P2VP. The PMMA $C_{1s}$ core levels are identified as follows. The carbonyl carbon appears at 3.5-eV higher binding energy than the primary peak which, in turn, arises from the three backbone carbons of the repeat unit. The ester carbon produces the shoulder appearing 1.5 eV above the primary peak. The relative intensity ratios for the carbonyl, ester, and backbone carbons are 1:1:3, respectively, which are characteristic of the repeat unit of PMMA. The $O_{1s}$ core level spectrum consists of a doublet derived from the double- and single-bonded oxygens. The double-bonded oxygen lies 1.5 eV lower in binding energy than the single-bonded oxygen.

These details of the homopolymer XPS spectra are specific enough to allow an unambiguous analysis of the surface composition of the Sty/MM and Sty/2VP copolymers.

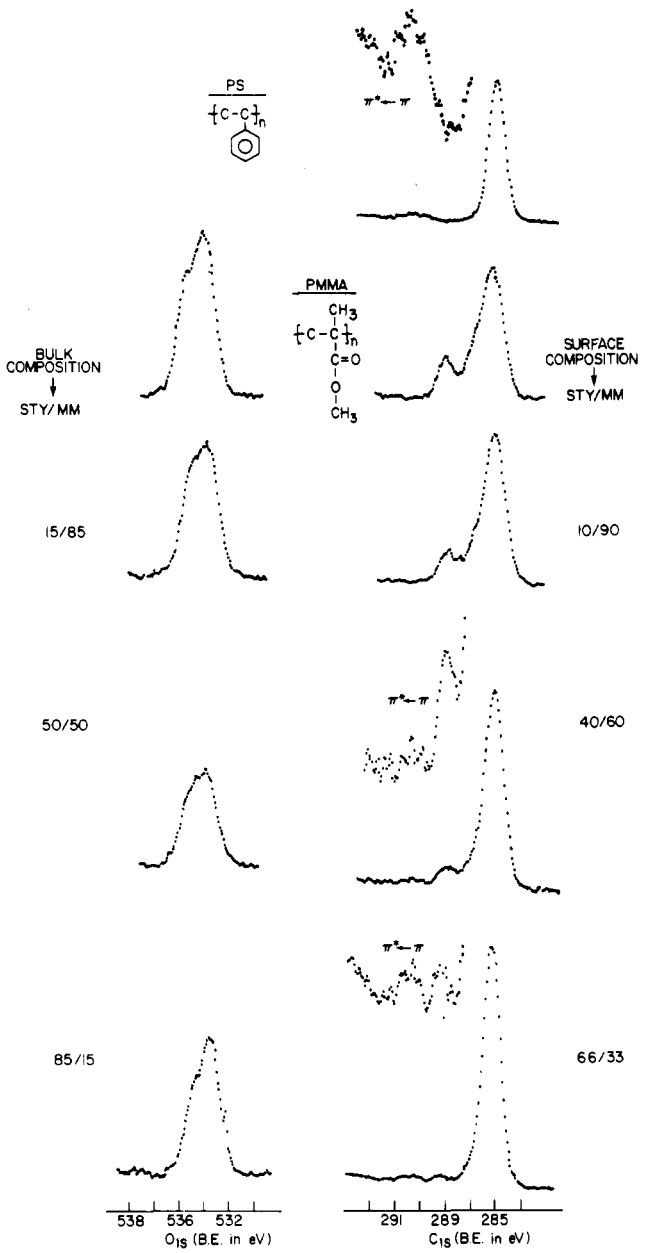


**Figure 1.** XPS($\theta$ = 0) core-level spectra for PS and PMMA homopolymers and Sty/MM copolymers of various bulk compositions.

The first application of the XPS spectra involves determining the surface composition of the random Sty/MM copolymer system for comparison to the nominal bulk composition. The Sty/MM ratio in the outermost surface region was calculated from the intensity ratios of the copolymer $C_{1s}$ core level spectra after applying curve resolution techniques and appropriate sensitivity factors deduced from the homopolymer spectra. The calculated surface Sty/MM ratios are tabulated at the right-hand side of Figure 1. It is clear that the surface concentration of Sty increases linearly in the progression from 15/85 Sty/MM to 85/15 Sty/MM but not as rapidly as in the bulk, as shown explicitly in Figure 3.

The XPS spectra also permit examination of the possibility of electronic interaction between the constituent moieties of the copolymers. A careful examination of the fine details of the $C_{1s}$ and $O_{1s}$ core level spectra for the Sty/MM system indicates that the individual components of the spectra are consistent with the details of the homopolymer spectra corrected for dilution to copolymer molar

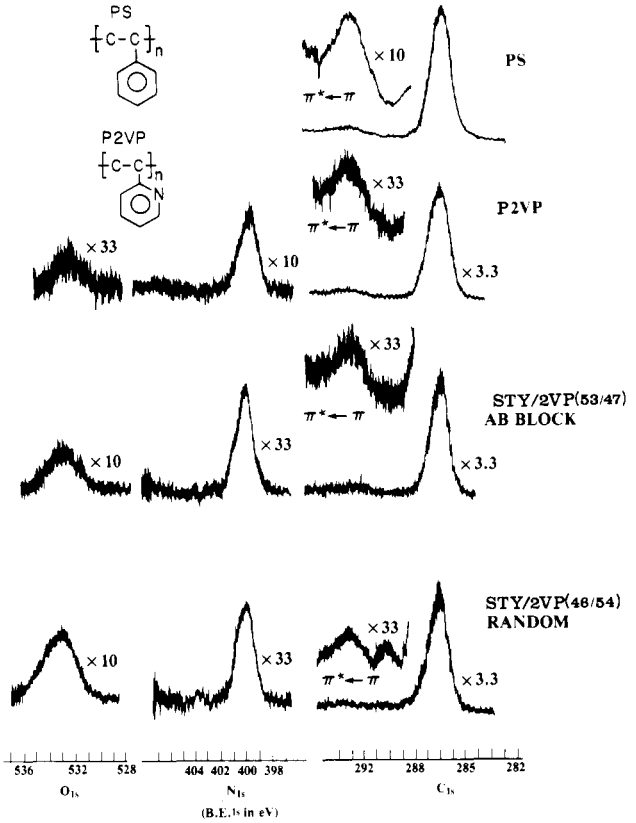


**Figure 2.** XPS($\theta$ = 0) core-level spectra for PS and P2VP homopolymers and block and random Sty/2VP copolymers.

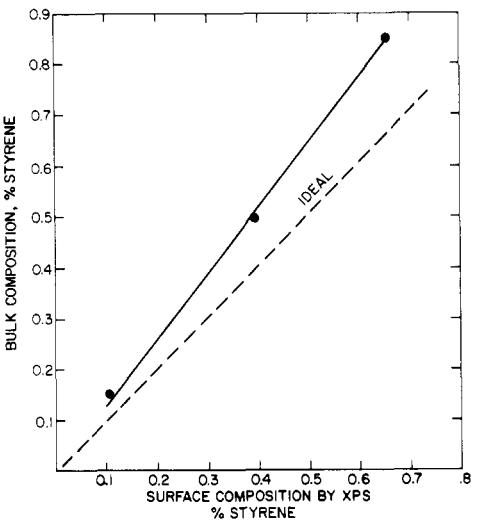


**Figure 3.** Surface composition of the random Sty/MM deduced from intensity analysis compared to nominal bulk compositions.

ratios. Hence, there is no spectroscopic evidence for an interaction (e.g., of a charge-transfer type) between the phenyl and ester pendent groups in the random Sty/MM copolymer system at any molar ratio studied.

The compositional data for the Sty/2VP copolymer system is found on the right-hand side of Figure 2. Unlike the Sty/MM system, the data for the block and random copolymers of Sty/2VP indicate some interesting surface phenomena. Considering first the block system, we note that the precise similarity of the respective $C_{1s}$ and $N_{1s}$ core level spectra to the homopolymer spectra indicates that both the Sty and 2VP components exist at the surface, probably as isolated homopolymer domains with no observable interaction between the domains. The surface appears to be somewhat enriched in 2VP, as the $C_{1s}$

spectrum from the block copolymer is nearly superimposable on the $C_{1s}$ spectrum for the P2VP homopolymer with no intensity correction for dilution.

In contrast to block Sty/2VP, as well as to random Sty/MM, the random Sty/2VP copolymer does not exhibit simple superposition of the characteristic constituent responses. The $C_{1s}$ $\pi^* \leftarrow \pi$ region of the spectrum (Figure 2) exhibits definite deviations from both the PS and P2VP homopolymer spectra. The first point to note is a broadening in the primary $C_{1s}$ peak in the random Sty/2VP copolymer (fwhm 2.0 ± 0.2 eV) relative to those in the PS (fwhm 1.5 ± 0.2 eV) and P2VP (fwhm 1.7 ± 0.2 eV) homopolymers. The primary peak encompasses the backbone and ring carbons of the polymer repeat unit. The relative intensities of the observed broadening are consistent with an approximately 0.2-eV shift of the ring carbons to higher binding energy in the random copolymer. The energy shift indicates that an alteration of the electronic structure of the pendent group occurs in the random copolymer configuration that is not observed in the block configuration.

Secondly, the asymmetry in the $C_{1s}$ $\pi^* \leftarrow \pi$ transition region of the PS homopolymer appearing at higher binding energy in Figure 2 is due to the electronic transitions, $b_{1\pi}^* \leftarrow b_{1\pi}$ and $b_{1\pi}^* \leftarrow a_{2\pi}$. These transitions are separated by only 0.8 eV and have intensities of 3.3% and 4.8%, respectively, relative to the signal due to atoms in and attached to the phenyl ring.[17-19] However, the shake-up peak associated with the random copolymer displays a distinct "doublet", rather than an asymmetric structure, and a significantly decreased intensity relative to the primary $C_{1s}$ core level peak.

Such line-shape and intensity changes were previously observed by Dilks and Clark[13,17-19] in para-substituted polystyrene. These workers showed that para substitution of strong $\pi$-electron donor or acceptor groups on the phenyl groups in polystyrene resulted in a significant perturbation of the asymmetry of the shake-up peak. Specifically, the centroids of the satellite structure were found to increase in energy separation with respect to the main $C_{1s}$ peak as the para substituent was changed from a $\pi$-electron donor to a $\pi$-electron acceptor. Moreover, the relative intensity of the $\pi^* \leftarrow \pi$ peak to the main $C_{1s}$ photoionization peak depended on the nature of the para substituent; the $\pi^* \leftarrow \pi$ peak intensity decreased with increasing electron-donating power of the para substituent.

While a direct correspondence of the nature of the interaction occurring in random Sty/2VP to that in the para-substituted polystyrenes is not warranted on the basis of available data, the similarities of the distortions found in the two polymer systems does suggest that the normal charge distribution for the phenyl group in PS may be altered by a charge-transfer interaction with the pyridine group in the random Sty/2VP configuration. A pendent-group interaction of this kind is absent in both the random Sty/MM and block Sty/2VP copolymers.

An oxygen impurity is clearly evident in the XPS spectra for the P2VP system in Figure 2. The presence of the oxygen in the form of an *N*-oxide might seriously alter the electronic structure of the pyridine pendent group and thus affect our conclusions regarding the phenyl-pyridine pendent-group interaction. Therefore, an evaluation of the nature and significance of the indicated oxide is necessary.

The $O_{1s}$ core level spectra in the P2VP homopolymer and block and random polymers in Figure 2 are centered at 533-eV binding energy, suggesting that the oxygen impurity is attached to a carbon. However, the fwhm of approximately 2.5 eV for this oxygen is quite large compared, for example, to the singly and doubly bound oxygens comprising the doublet in PMMA (Figure 1). The extended breadth of the oxygen-impurity signal in the 2VP polymers is probably indicative of oxygen present in varying electronic environments.

The symmetry of the $N_{1s}$ peak in P2VP also suggests an insignificant contribution from *N*-oxide. Moreover, there is no clear evidence from distortions in the $C_{1s}$ primary peak for carbon bound to oxygen. The absence of a significant oxygen-induced perturbation in the $C_{1s}$ spectrum and the reduced magnitude of the $O_{1s}$ signal relative to the $C_{1s}$ signal despite the larger theoretical photoionization cross section for oxygen core level electrons ($O_{1s}/C_{1s}$ = 2.85) are consistent with confinement of the oxygen impurity to the outermost surface layers of the polymer films. Indeed, angular-distribution measurements, XPS($\theta$) (not shown), revealed the $O_{1s}$ signal to increase as $\theta \rightarrow 90°$, as expected for surface features. In contrast, the alterations in the $\pi^* \leftarrow \pi$ shake-up spectrum for the random Sty/2VP copolymer noted previously were found to be independent of the exit angle, $\theta$, which is characteristic of features that are uniform throughout the XPS sampling depth.[9]

Available evidence thus favors viewing the oxygen impurity as associated with a carbon lying in the near-surface region of the film. Its presence is apparently benign with regard to the alterations in the $C_{1s}$ primary peak and $\pi^* \leftarrow \pi$ shake-up spectrum observed in the random Sty/2VP configuration relative to these responses in the block configuration and homopolymer.

The XPS($\theta$) spectra (not shown) for both the Sty/MM and Sty/2VP copolymer systems showed little dependence upon sampling depth (i.e., on $\theta$), except for the oxygen-impurity response discussed previously. This result indicates[9] that the constituent moieties of these copolymers are randomly dispersed throughout the XPS depth-profiling scale of approximately 100 Å.

## Contact Charge Exchange

**A. Experimental Procedure.** The injection of charge from metals into polymer films taking place during contact of the metal to the polymer is known[1,2] to be dependent upon the polymer chemical structure. The response from such a contact-charging experiment is specific enough to certain polymer repeat units to constitute a sensitive analytical probe of copolymer electronic structure.

The contact-charging experiments involve repeatedly contacting a flat metal disk to a flat, solvent-cast polymer film with no applied bias potential until the film potential associated with the charge injected into the polymer during contact reaches a steady-state value. Details of these experiments are reported elsewhere.[1] Here we note the film preparation is important (purified resins and solvents, vacuum drying, and control over environment during heating of the films in the course of the experiments), as is experimental technique to achieving reproducibility and to ensure that the results reflect intrinsic polymer charge states.

Measurement of the surface potential of the charged and charge-neutral films was performed by a standard noncontacting technique.[1] For the charge-neutral film, the result of this measurement is the contact potential difference (CPD) between the metal and polymer film. The CPD values for the various homopolymers and copolymers relative to a gold reference (work function of 4.3 eV) are important for the detection of surface orientation in the polymers. The important variables in the contact-charging experiments are film thickness and the contacting metal. Varying the film thickness provides information about the spatial distribution of the injected charge.[1,2] This aspect

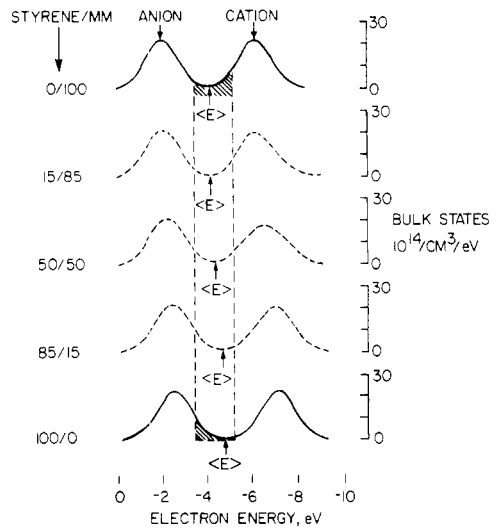


**Figure 4.** Gaussian representations of the solid-state anion and cation states of polystyrene and poly(methyl methacrylate) and selected molar-weighted superpositions of the homopolymer spectra. The double-Gaussian fits to the experimental homopolymer contact-charging data, which in itself covers the energy interval −3.0 to −5.5 eV, as indicated by the hatched areas under the curves, are specified by their peak positions, half-width, and normalization. The experimental results for PS and PMMA (in parentheses) are adequately represented by Gaussians having the following parameters: $E$(anion peak) = −2.5 eV (−2.0 eV), $E$(cation peak) = −7.1 eV (−6.1 eV), half-width = 0.845 eV (0.845 eV), centroid $\langle E \rangle$ = −4.8 eV (−4.1 eV); state densities are normalized to $4 \times 10^{15}$ states/cm$^3$ in both cases. The molar-weighted spectra constitute predictions of the contact-charging experimental results for random copolymers based upon the idea of molecular superposition of the distinctive charge localization sites (the phenyl group and appended structure comprising the repeat unit of PS and the oxygen lone-pair orbitals in the ester group in the repeat unit of PMMA, respectively).

of the experiment will not concern us here except to note that the typical penetration depth of the injected charge corresponding to the steady state is about 2 μm. Because the injection from metals into polymer charge states has been shown to be keyed to the Fermi level of the metal, the use of metals covering a range of work functions provides a means to resolve in energy the distribution of polymer charge states.[1,2] It is the ability to distinguish the polymer charge-state distribution that provides the requisite sensitivity in the investigation of copolymer electronic structure via charge injection.

**B. Results.** A clear signal in the metal/polymer contact experiments corresponds to a large injected charge (≥3 nC/cm$^2$) or change in sign of the injected charge for different metallic contacts. For the homopolymers PS, PMMA, and P2VP, maximum signal was typically obtained with the lowest work function metal employed in the contacts (In) and/or the highest (Sn). The investigation of the electronic structure of copolymers incorporating any two of these repeat units proceeds by comparing the injected charge levels for these particular metallic contacts for the homopolymers and copolymers. In addition, the full molecular ion distributions deduced from the contact experiments provide values for the polymer chemical potential[2] that can be compared to the CPD measurements of this quantity. Since the former is bulk sensitive (contact-injected charge penetrates to 2 μm) and the latter surface sensitive, information about orientation effects and pendent-group interactions may be discerned.

We discuss first the styrene/methyl methacrylate (Sty/MM) copolymer system as an example where the pendent-group-governed electrical characteristics of the

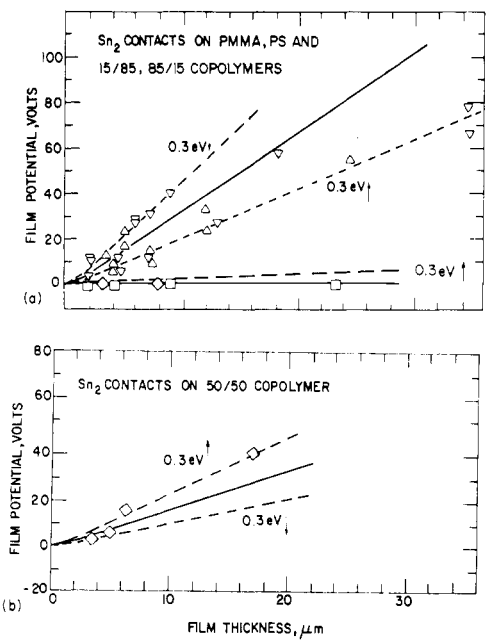


**Figure 5.** Comparison of the predicted charge exchange for styrene/methyl methacrylate copolymers with experiment. The steady-state film potentials for Sn contacts on the 15/85 copolymer (△) are seen in panel a to be indistinguishable from 0/100 (▽), and the results for the 85/15 copolymer (□) are indistinguishable from 100/0 (◇) within the uncertainty in the molecular ion representation (the solid and dashed curves). According to the superposition hypothesis for noninteracting pendent-group polymers, Sn contacts to the 50/50 copolymer should be represented by $^1/_2$ the sum of the values for the homopolymers given in panel a (eq 1). The data for the 50/50 copolymer, panel b, are seen to be consistent with this prediction.

homopolymers superpose. Here we essentially summarize a previous discussion.[2,8]

The molecular ion distributions for the PS and PMMA homopolymers deduced from metal/polymer contact-charging experiments are given in Figure 4. Also shown in Figure 4 are various molar-weighted superpositions of the two homopolymer spectra. These hypothetical copolymer spectra were tested by performing contact experiments on the copolymers. Because PS and PMMA differ little, 0.8 eV, in chemical potential[2] ($\langle E \rangle$ in Figure 4), only the 50/50 copolymer can be expected to show significant differences in contact charge exchange behavior from one or the other homopolymers. That is, in progressing from PS, for which only anion states are accessed in metallic contacts, we note (Figure 4) that cation states first reach some degree of prominence at energies corresponding to the higher metallic work functions at 50/50 composition. Hence, we expect the 85/15 Sty/MM copolymer to be indistinguishable from PS and the 15/85 copolymer to be indistinguishable from PMMA (which was shown to be the case). For the 50/50 composition, however, high work function metallic contacts (Sn in the present case) are predicted by molecular superposition to result in a positive charge density half that observed for PMMA.

The contact-charging results for Sn contacts on PS and PMMA and the 85/15, 15/85, and 50/50 copolymers are shown in Figure 5. The results are seen to agree with the predictions from the superposition spectra. We conclude that the phenyl and ester pendent groups that distinguish the homopolymers act independently in the random copolymer configuration to a similar degree as in the homopolymers within the spatial region probed by the injection experiments. This finding is in essential agreement with the observation of superposition of XPS spectra in this

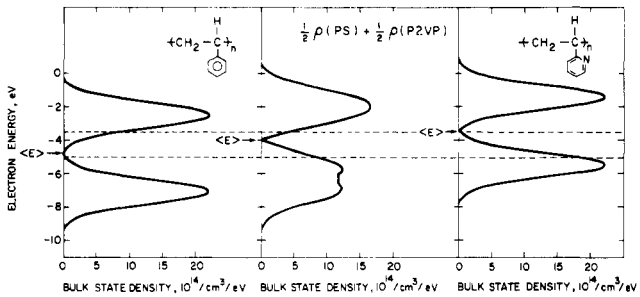


**Figure 6.** Gaussian representations of the solid-state anion and cation states of polystyrene and poly(2-vinylpyridine) and a molar-weighted 50/50 superposition of the homopolymer spectra. The Gaussian parameters for PS were given in Figure 4. Those for P2VP are $E$(anion) = −1.4 eV, $E$(cation) = −5.5 eV, half-width = 0.845 eV, $\langle E \rangle$ = −3.4 eV. The normalization is defined to yield $4 \times 10^{15}$ states/cm$^3$. The contact-charging experiments provide state-density information in the energy region lying between the horizontal dashed lines.

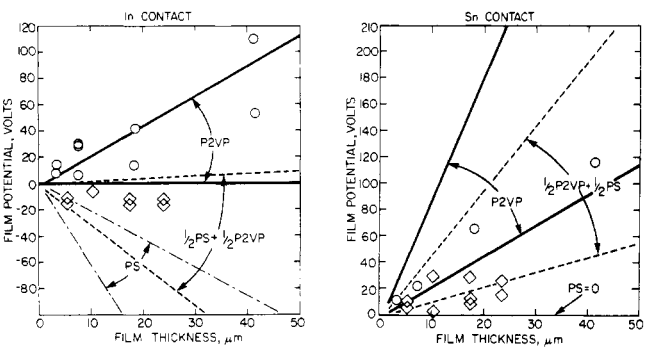


**Figure 7.** Comparison of the predicted charge exchange for styrene/2-vinylpyridine block and random copolymers with experiment. The steady-state film potentials for indium and tin contacts (the largest signal cases) to 46/54 random (○) and 53/47 block (◇) copolymer films are compared to the relevant boundary curves for the homopolymers and for the predicted copolymer response, assuming superposition (eq 1). It is seen that the block copolymer falls in the range described by superposition, while the random configuration responds similarly to the P2VP homopolymer for both metallic contacts.

copolymer system discussed previously.

The Sty/2VP copolymer system can be investigated by the same techniques. The full molecular ion distributions for PS[2] and P2VP[7] deduced from the complete series of contact-charging experiments are given in Figure 6, along with a molar-weighted superposition of these spectra corresponding to a 50/50 copolymer. The steady-state contact-charging results obtained on thermally stabilized films for the lowest and highest work function metals, In and Sn, respectively, for the 46/54 Sty/2VP random and 53/47 block copolymers investigated herein are given in Figure 7. These data are to be compared to the extremal curves[2] describing the range of film potential realized for these metal contacts on the homopolymers, as well as to the bounding curves corresponding to molar-weighted superposition of the homopolymer responses, as calculated from the charge-state distribution given in Figure 6. The latter calculation proceeds according to eq 1, where $\rho_i(E)$

$$\rho(E) = \chi\rho_1(E) + (1 - \chi)\rho_2(E) \qquad (1)$$

is the (measured) homopolymer charge-state density and $E$ the (electron) energy; $\rho(E)$ is the calculated charge-state density for a copolymer comprised of molar fraction $\chi$ of homopolymer 1 and $1 - \chi$ of homopolymer 2. In the present system, homopolymer 1 is PS, and 2 is P2VP, while $\chi = {}^1/_2$. The experimental observable in the contact experiment is the steady-state film potential, $\Delta V$, which is proportional to $\rho(E)$ in our approximation.[1,2] Hence, the experimental $\Delta V$ values for the copolymer films are to be compared with the curves given by $\Delta V$(Sty/2VP) = ${}^1/_2\Delta V$(PS) + ${}^1/_2\Delta V$(P2VP) to evaluate the relevance of superposition. The appropriate boundary curves for the homopolymers[2,7] and the hypothetical curves representing superposition of the homopolymer responses are given in Figure 7.

Comparison of the steady-state film potentials for the random and block Sty/2VP copolymer films with the homopolymer and superposition boundary curves in Figure 7 shows that superposition describes well the block copolymer but not the random copolymer which clearly responds similarly to the homopolymer P2VP. The latter indicates that either the surface of the random Sty/2VP copolymer is dominated by the 2VP moiety or that the phenyl and pyridine pendent groups interact throughout the bulk to alter the chemical potential of the copolymer. In addition, the striking difference in behavior of the random and block copolymers suggests an important effect of physical structure on the electronic structure of this copolymer system.

**C. Discussion.** Independent response of the distinct molecular ion sites clearly will depend upon the degree of electronic interaction existing between adjacent pendent groups. This, in turn, will depend upon the strength of the thermodynamic drive for interaction and the physical proximity of the distinct sites. The results for the Sty/MM and Sty/2VP copolymer systems can be employed to provide insight into the molecular interactions and geometric constraints active in copolymer structures.

An estimate of the thermodynamic drive for electronic interactions between the distinct pendent groups may be obtained from the homopolymer molecular ion distributions (Figures 4 and 6). The polymer chemical potential has been identified[2] with the distribution centroid, $\langle E \rangle$. The drive for stronger pendent-group interaction may thus be expected to scale with increasing differences between the constituent homopolymer $\langle E(i) \rangle$. For Sty/MM, $\Delta\langle E \rangle$ = 0.8 eV (Figure 4), while for Sty/2VP, $\Delta\langle E \rangle$ = 1.4 eV (Figure 6).

The copolymer structure most favorable to pendent-group interaction is the random configuration. While the "random" structure may actually include segments consisting entirely of a single moiety, these are insufficient to permit the formation of extensive domains consisting of a single moiety. The random structure thus ensures the closest approach of the distinct pendent groups' structures and their maximum alternation throughout the sample volume. The charge-injection results for the random configurations may be interpreted, then, as manifestations of an insignificant interaction present in the Sty/MM system, where molecular superposition is observed, while loss of superposition in random Sty/2VP indicates a very significant pendent-group interaction. Expressed in terms of the $\Delta\langle E(i) \rangle$ from the homopolymer spectra, pendent-group interaction becomes significant only when $\Delta\langle E \rangle$ exceeds 0.8 eV, and certainly by $\Delta\langle E \rangle$ = 1.4 eV.

Consistent with a strong thermodynamic drive for interaction, the superposition observed for the block Sty/2VP copolymer configuration is interpreted as reflecting the presence of important geometrical constraints on pendent-group interaction. That is, superposition in the block configuration is a manifestation of the formation of domains comprised largely of each constituent moiety, a common occurrence in incompatible block systems. Domain formation relegates the interaction between the phenyl and pyridine groups to the domain interface. This

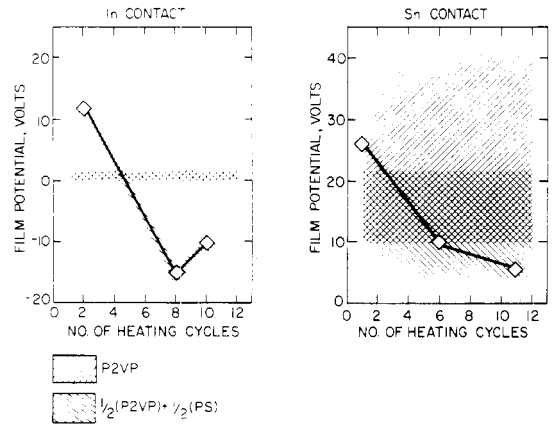


**Figure 8.** Thermal history of the steady-state film potentials for indium and tin contacts on a 5.5-μm-thick, 53/47 Sty/2VP block copolymer film. The response is initially similar to that of P2VP but comes to follow superposition of the homopolymer responses after sufficient exposure to elevated temperatures. A typical heating cycle employed to discharge a contact-charged film consists of holding the film approximately 15 min above $T_g$ ($T_g$ = 100 °C for PS and P2VP) followed by slow cooling to room temperature. Consideration of the other metallic contacts besides those shown indicates that the equilibrium block structure is attained after the second heating cycle.

would have the effect of leaving the electronic states of the two distinct moieties relatively unperturbed throughout most of the sample volume, as observed in both the charge-injection and photoemission experimental results. Hence, superposition in the block Sty/2VP copolymer is visualized to result from an area-averaging effect related to the presence of large, essentially homopolymer domains, as opposed to superposition at the molecular level as occurs in the noninteracting Sty/MM random copolymer system.

It is interesting to note that superposition in the block Sty/2VP system became established in these experiments only after a period of time elapsed following film preparation. In the performance of the contact experiments, the polymer film that has been charged by metallic contacts is returned to a charge-neutral state for reuse by heating the film (under vacuum) above its $T_g$. The history of the steady-state film potentials for In and Sn contacts on a particular block Sty/2VP film is given in Figure 8. It is seen that the block begins by responding like P2VP, similarly to the random copolymer. The initial state of the copolymer film may be expected to be sensitive to the film-preparation technique,[1] e.g., the solvent used. Only after two heating cycles does the block begin to reflect the styrene moiety. The data in Figure 8 suggest that creation of the final, equilibrium copolymer surface in the block Sty/2VP system proceeds slowly and may require the higher molecular mobilities available at elevated ($>T_g$) temperatures. The contact-charging results for the block copolymer employed in Figure 7 are those obtained on the thermally stabilized films. As the XPS specimens were heated about 1 h above the polymer $T_g$ under vacuum prior to the measurements, it is expected that the XPS results of Figures 1–3 also correspond to equilibrium physical structures.

**D. Surface Structure.** The charge-injection experiments reflect bulk electronic structure, while photoemission spectra give detailed information about the first few monolayers of the polymer surface. The photoemission results for the homopolymers and copolymer systems studied in this work gave no indication of peculiar surface effects, such as the presence of dipole layers arising from molecular orientations at the vacuum/polymer interface. However, the combination of CPD measurements and

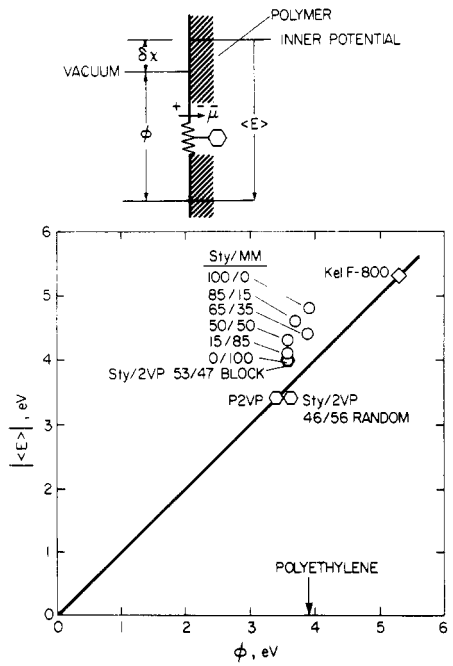


**Figure 9.** Correlation of the polymer surface potential, $\phi$, with the polymer (bulk) chemical potential, $\langle E \rangle$. $\phi$ is defined as the negative of the measured contact potential difference, using a gold reference (work function 4.3 eV). $\langle E \rangle$ is defined as the centroid of the polymer molecular ion distribution deduced from contact-charging experiments. A 1:1 correlation (solid line) implies similar surface and bulk structures. (The CPD of polyethylene was measured, as shown, but charge could not be injected into clean polyethylene in metallic contacts, thus precluding measurement of $\langle E \rangle$.)

charge-injection experiments does suggest dipole-layer formation in certain cases. Because of the differing sensitivities of the photoemission and CPD/injection experiments to surface structure, it is worth considering the latter results further in the spirit of perhaps providing a basis for potentially useful correlations with other kinds of experimental results.

The polymer chemical potential has been identified with the centroid, $\langle E \rangle$, of the molecular charge-state distributions.[2] It can be expected that $\langle E \rangle$ determined in this way should, in the absence of surface dipole layers, bear a definite relationship with the measurement of this quantity obtained from the CPD measurement,[1,2] designated $\varphi$ herein. The relationship for several homopolymers and copolymers is given in Figure 9.

It is instructive to interpret the deviations of individual points from the ideal 1:1 correlation indicated in Figure 9 in terms of a surface dipole layer whose origin lies in orientation of the bond dipole moments of the pendent groups. Because the charge-injection experiments comprise a relatively deep (2 μm) probe of the polymer electronic structure, $\langle E \rangle$ should represent the polymer chemical potential independent of surface orientation effects. Hence, the progressively larger deviations of $\varphi$ from $\langle E \rangle$ in the series of homopolymers and copolymers including (block) Sty/2VP, PMMA, Sty/MM, and PS correspond, in this model, to progressively stronger and/or denser molecular dipoles pointing into the bulk, as shown schematically in Figure 9. The deviation of the random Sty/2VP copolymer is opposite to the others but the magnitude of the deivation from P2VP and the 1:1 correlation is quite small. No surface orientation effects are suggested for P2VP.

The density of the pendent groups in these polymers is approximately $6 \times 10^{21}$ cm$^{-3}$, giving an average surface

density of $4 \times 10^{14}$ cm$^{-2}$. The dipole moment of the repeat unit of PMMA associated with the pendent ester group is 1.3 D.[20] Approximately $1 \times 10^{14}$ molecular dipoles of this strength oriented into the bulk would account for the observed 0.4-eV shift in $\phi$ below $\langle E \rangle$ for PMMA. Similarly, assuming a dipole strength of 0.36 D as representative of PS,[20] the observed 0.9-eV deviation in $\phi$ from $\langle E \rangle$ requires a dipole density of $8 \times 10^{14}$ cm$^{-2}$. For both PS and PMMA, and thus their copolymers, there is approximate agreement between the available dipole density and that required to account for the observed deviation in surface potential from the bulk chemical potential. The implication is a slightly aliphatic surface for PMMA and a strongly aliphatic surface for PS. Our XPS($\theta$) studies were not extensive enough to directly detect the presence or absence of pendent-group orientation at the surface.

A major uncertainty in the interpretation of the CPD and $\langle E \rangle$ measurements in terms of dipole strengths and coverages lies in the oversimplification of characterizing the surface dipole layer by a uniform layer of model polymer repeat units. For example, the ester pendent group of PMMA may assume a variety of configurations at the interface,[21] each having a different net dipole moment. In general, then, there exists a distribution of moments which result in the net alteration in surface potential indicated by the $\phi$–$\langle E \rangle$ correlation, and not all of these moments are known from measurements on model systems.

Whatever the interpretation of the deviations of $\phi$ from $\langle E \rangle$ appearing in Figure 9, the correlation clearly shows that the variation within the Sty/MM system of copolymers is monotonic between the homopolymer limits. This is consistent with molecular superposition at all molar ratios as deduced from the contact charge injection and photoemission experiments, although the surface enrichment of MM witnessed in the XPS spectra is not discernible in Figure 9. The correlation also indicates that the equivalence of the random Sty/2VP copolymer to P2VP seen in the bulk via the charge-injection experiments is maintained to the surface (equal $\phi$'s as well as equal $\langle E \rangle$'s for random Sty/2VP and P2VP), as must occur for the interaction to appear in the XPS spectra. Finally, homopolymer domains in the 50/50 block Sty/2VP copolymer are manifested in Figure 9, as expected, in their approximately equal representation in determining the copolymer $\langle E \rangle$ and $\phi$ (within the experimental uncertainities of $\pm 0.3$ eV in $\langle E \rangle^2$ and $\pm 0.2$ eV in $\phi^1$). That such structure continues to the surface of this block copolymer was previously verified by XPS.

## Summary

X-ray photoemission and contact-charge experiments performed on PS and PMMA homopolymers and Sty/MM random copolymers were found to be in essential agreement in demonstrating in the random copolymer the existence of superposition of the characteristic phenyl and ester pendent-group electronic responses that govern the lowest energy homopolymer excitations. In a second example, a random copolymer incorporating phenyl and pyridine pendent groups exhibited a pendent-group interaction that effectively eliminated the characteristic phenyl-group response in favor of the pyridine-group response. In contrast, a block copolymer comprised of large alternating segments of phenyl and pyridine groups preserved the individual responses of the two groups. The unifying concept that allows interpretation of these results is the requirement of both a sufficiently large thermodynamic drive for pendent-group interaction, which is determined by the electronic structures of the groups, and an appropriate copolymer geometry that permits close enough approach of the two electronic structures to allow a charge-transfer interaction to occur. Hence, insufficient thermodynamic drive exists in the random Sty/MM system to significantly alter the constituent electronic structures, while the formation of domains of phenyl and pyridine groups in the block Sty/2VP configuration prohibits extensive, thermodynamically favored pendent-group interaction. The geometric constraint is lifted in the random Sty/2VP configuration and pendent-group interaction duly occurs. While the series of three copolymers illustrates the concepts as well as the rather striking observable effects possible in interacting copolymers, the exact manifestations of the interaction in photoemission spectra and charge-injection response are presently not predictable.

**Acknowledgment.** We thank Dr. Thomas W. Smith and John G. Van Dusen for synthesizing the polymers utilized in this work, Dr. James J. O'Malley for support and advice, and Barbara Fornalik for assistance.

## References and Notes

(1) Fabish, T. J.; Saltsburg, H. M.; Hair, M. L. *J. Appl. Phys.* **1976**, *47*, 930, 940.
(2) Fabish, T. J.; Duke, C. B. *J. Appl. Phys.* **1977**, *48*, 4256.
(3) Duke, C. B.; Fabish, T. J. *Phys. Rev. Lett.* **1976**, *37*, 1075.
(4) Duke, C. B.; Fabish, T. J.; Paton, A. *Chem. Phys. Lett.* **1977**, *49*, 133.
(5) Duke, C. B. *Surf. Sci.* **1978**, *70*, 674.
(6) Duke, C. B. *Mol. Cryst. Liq. Cryst.* **1979**, *50*, 63.
(7) Duke, C. B.; Salaneck, W. R.; Fabish, T. J.; Ritsko, J. J.; Thomas, H. R.; Paton, A. *Phys. Rev. B* **1978**, *18*, 5717.
(8) Duke, C. B.; Fabish, T. J. *J. Appl. Phys.* **1978**, *49*, 315.
(9) Thomas, H. Ronald; O'Malley, J. J. *Macromolecules* **1979**, *12*, 323.
(10) Siegbahn, K.; Nordling, C.; Fahlman, A.; Nordberg, R.; Hamrin, K.; Hedman, J.; Johansson, G.; Berkmark, T.; Karlsson, S. E.; Lindgren, I.; Lindberg, B. "ESCA, Atomic, Molecular and Solid State Structure Studied by Means of Electron Spectroscopy"; Almquist and Wiksells: Uppsala, 1967.
(11) Clark, D. T. In "Electron Emission Spectroscopy"; Dekeyser, W., Fiermans, L., Vander Kelen, G., Vennik, J., Eds.; D. Reidel Publishing Co.; Dordrecht, Holland, 1973; pp 373–507 (NATO Summer School Lectures, Ghent, Sept 1972).
(12) Clark, D. T. In "Electronic Structure of Polymers and Molecular Crystals"; Andre, L. J., Ladik, J., Delhalle, J., Eds.; Plenum Press: New York, 1975; pp 259–387.
(13) Clark, D. T. In "Advances in Polymer Science"; Cantow, H. J., et al., Eds.; Springer-Verlag: Berlin, 1977; pp 126–88.
(14) Clark, D. T.; Thomas, H. R. *J. Polym. Sci., Polym. Chem. Ed.* **1977**, *15*, 2843.
(15) Clark, D. T.; Thomas, H. R.; Dilks, A.; Shuttleworth, D. *J. Electron Spectrosc.* **1977**, *10*, 455.
(16) Clark, D. T.; Thomas, H. R. *J. Polym. Sci., Polym. Chem. Ed.* **1976**, *14*, 1671.
(17) Dilks, A. Ph.D. Thesis, University of Durham, U.K., 1977.
(18) Clark, D. T.; Dilks, A. *J. Polym. Sci., Polym. Chem. Ed.* **1976**, *14*, 533.
(19) Clark, D. T.; Dilks, A. *J. Polym. Sci., Polym. Chem. Ed.* **1977**, *15*, 15.
(20) Brandrup, J., Immergut, E. H., Eds. "Polymer Handbook", 2nd ed.; Wiley: New York, 1975; pp IV 320–1.
(21) Osipow, L. I. "Surface Chemistry"; Reinhold: New York, 1963; p 104.